

AD-A092 955

NAVAL RESEARCH LAB WASHINGTON DC F/G 9/1

POWER LIMITS IN CYLINDRICAL GYROMONOTRONS USING TEONL MODES. (U)

NOV 80 M E READ, K R CHU, K J KIM

DE-AC01-79-ET-52053

UNCLASSIFIED

NRL-MR-4349

NL

1-12
ALL
GROWING



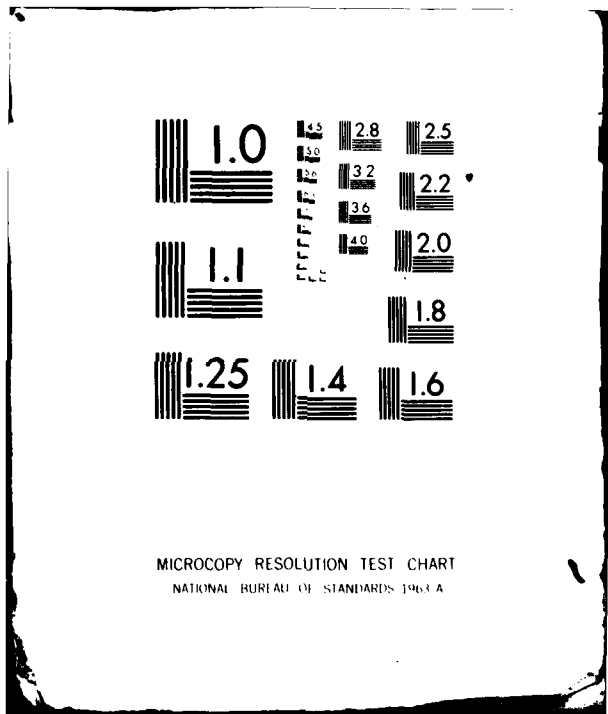
END

DATE

FILED

1 81

DTIC



AD A092955

15

DE-AC01-79-ET-52053

SECURITY CLASSIFICATION OF THIS PAGE (When Data Entered)

REPORT DOCUMENTATION PAGE		READ INSTRUCTIONS BEFORE COMPLETING FORM	
1. REPORT NUMBER	2. GOVT ACCESSION NO.	3. RECIPIENT'S CATALOG NUMBER	
NRL Memorandum Report 349	AD-A092955		
4. TITLE (and Subtitle)	5. TYPE OF REPORT & PERIOD COVERED		
6. POWER LIMITS IN CYLINDRICAL GYROMONOTRONS USING TE ₀₁₁ MODES.	Interim report on a continuing NRL problem		
7. AUTHOR(s)	6. PERFORMING ORG. REPORT NUMBER		
10. M.E. Read K.R. Chu and K.J. Kim	14	7. CONTRACT OR GRANT NUMBER(s)	
8. PERFORMING ORGANIZATION NAME AND ADDRESS	10. PROGRAM ELEMENT, PROJECT, TASK AREA & WORK UNIT NUMBERS		
Naval Research Laboratory Washington, DC 20375	NRL Problem 67-0865-0-0 DOE No. DE-AC01-79ET52053		
11. CONTROLLING OFFICE NAME AND ADDRESS	11	12. REPORT DATE	
Department of Energy Washington, DC 20585		13. NUMBER OF PAGES	
14. MONITORING AGENCY NAME & ADDRESS (if different from Controlling Office)	12	15. SECURITY CLASS. (of this report)	
	26	Unclassified	
16. DISTRIBUTION STATEMENT (of this Report)	15a. DECLASSIFICATION/DOWNGRADING SCHEDULE		
Approved for public release; distribution unlimited.			
17. DISTRIBUTION STATEMENT (of the abstract entered in Block 20, if different from Report)			
18. SUPPLEMENTARY NOTES			
*JAYCOR, Alexandria, VA			
19. KEY WORDS (Continue on reverse side if necessary and identify by block number)			
Gyrotron Cyclotron Maser mm Waves			
20. ABSTRACT (Continue on reverse side if necessary and identify by block number)			
Upper and lower limits to the output power of highly efficient gyrotron oscillators operating with TE ₀₁₁ modes, due to lower and upper limits on the cavity Q, are given.			

DD FORM 1 JAN 73 1473

EDITION OF 1 NOV 65 IS OBSOLETE

S/N 0102-014-6601

SECURITY CLASSIFICATION OF THIS PAGE (When Data Entered)

251950

CONTENTS

INTRODUCTION	1
UPPER LIMITS ON THE OUTPUT	1
LOWER LIMITS ON THE OUTPUT POWER	5
COMPARISON TO EXPERIMENT	6
COMMENTS	7
CONCLUSIONS	7
ACKNOWLEDGMENTS	8
REFERENCES	8

POWER LIMITS IN CYLINDRICAL GYROMONOTRONS USING TE_{on1} MODE

INTRODUCTION

Gyrotron oscillators (gyromonotrons) are of great interest as sources of high power mm-wave radiation for heating and preionization in fusion devices.⁽¹⁻³⁾ The total radiation power required for reactor size devices has been estimated at 50 - 100 MW⁽⁴⁾ at ~ 150 GHz, far beyond the present state of the art for a single source.⁽⁵⁾ Since the feasibility and cost of a heating system may be strongly dependent on the number of devices required, it is of interest to estimate the upper limit of the output power of a single gyromonotron. In this note we present calculations for such an estimate. In addition, we determine the lower limit on output powers. The detailed calculations are limited to right circular cavities supporting TE_{on1} modes, but some of the results are directly applicable to other geometries. All calculations are for devices operating near the cyclotron frequency, with a beam energy of 70 keV and negligible velocity spread.

UPPER LIMITS ON THE OUTPUT POWER

1. Optimum RF Field Amplitudes and Upper Power Limits Due to a Lower Limit to Q

As has been shown in a previous paper,⁽⁶⁾ the electronic efficiency of a gyromonotron is a function of the RF field local to the beam; thus the electronic efficiency (i.e., the basic interaction efficiency) is independent of the radial mode number n . For a given length of the cavity there will be a fixed RF field strength (at the beam location) for optimum efficiency, which we determine below. Once this field magnitude is known, and the cavity and beam properties given, the resulting output power can be predicted.

We start with the definition of Q :

$$Q \equiv \frac{2\pi f W_F}{P_w} \quad (1)$$

where f is the operating frequency, W_F the RF energy stored in the cavity, and P_w the RF power coupled out of and dissipated into the walls of the cavity. For a TE_{0n1} mode in a right circular cavity of length L and radius a ,

$$E_\theta = E_0 J_1 \left(\alpha_{1n} \frac{r}{a} \right) \sin \left(\frac{\pi}{L} \right) \cos \omega t, \quad (2)$$

and

$$W_F = \frac{\epsilon}{2} \int E_\theta^2 dV \quad (3)$$

where J_1 is a Bessel function of the first kind. In principle, the upper limit for P_w will be given, for a fixed E_θ , by the lower limit for Q , namely the diffraction Q given by ⁽⁷⁾

$$Q_D = 4\pi \left(\frac{L}{\lambda} \right)^2 \quad (4)$$

where λ is the free space wavelength. In practice, however, $2 \cdot Q_D$ is a reasonable lower limit to Q .

Using this value for Q , we obtain

$$P_w = \frac{c\epsilon_0\pi}{16} \frac{\lambda}{L} a^2 J_1^2(\alpha_{1n}) E_0^2. \quad (5)$$

α_{1n} is the n^{th} zero of $J_1(x)$.

Letting

$$E_0 = \frac{f g_b}{J_1(\alpha_{1n} \frac{b}{a})} \quad (6)$$

where g_b is the electric field at the beam location, normalized to the frequency, and b is the average beam radius, we obtain

$$P_w = \frac{c^3 \epsilon_0 \pi}{16} \frac{\lambda}{L} \frac{a^2}{\lambda^2} \frac{J_1^2(\alpha_{1n})}{J_1^2(\alpha_{1n} \frac{b}{a})} g_b^2. \quad (7)$$

Gyromonotron cavities are operated close to cut-off. Then:

$$\frac{a}{\lambda} \approx \frac{\alpha_{1n}}{2\pi}. \quad (8)$$

Substituting, we obtain

$$P_w = \frac{\epsilon_0 c^3}{64\pi} \alpha_{1n}^2 \frac{\lambda}{L} \frac{J_1^2(\alpha_{1n})}{J_1^2(\alpha_{1n} \frac{b}{a})} g_b^2 \quad (9)$$

g_b is a function of only L/λ , since it is normalized to the frequency. From computer calculations,⁽⁶⁾ the values of g_b , which yield the optimum efficiency, for a given length were found. These values are given in Fig. 1. The results of calculations for two values of α , the ratio of the perpendicular to parallel beam velocities, with and without magnetic tapering, are included in the figure. The efficiencies achievable for the various parameters are given in Fig 2, reproduced from Reference (6).

Using Eq. (9) and Fig. 1, the power obtainable at maximum efficiency is calculated and shown in Figs. 3a, b, c, and d.

These calculations assume that the beam is located at the peak of the first maximum of E_θ . From Eq. (9), and Table 1, it can be seen that higher powers can be obtained by operating with the beam on a higher order peak, and/or off of local maximum. Calculations show that, in the absence of mode competition, the efficiency remains essentially unchanged for $(E_\theta)_{beam} \geq \frac{1}{2} (E_\theta)_{peak}$, where $(E_\theta)_{peak}$ is the *local* maximum. Thus, enhancement of the output power by a factor of 4 is possible by operating with the beam off a local maximum and, additionally, by the factors given in Table 1, by placing the beam near the higher order peaks. As an example, approximately 500 kW could be generated using the TE_{051} mode, with the beam on the 4th peak, and 2 MW would be possible by offsetting the beam to the limit of $E_\theta = \frac{1}{2} (E_\theta)_{peak}$. We note that these calculations assume that only the mode of interest would be excited. If other modes (such as whispering gallery modes)⁽⁸⁾ have absolute maxima at the beam position, these modes may then be more readily excited, and degrade or totally eliminate the efficiency of the TE_{on1} mode of interest.

2. Power Limits Due to Ohmic Losses

Ohmic losses in the cavity walls will cause reduced efficiencies and, at high average power, heating problems. We therefore calculate these losses, and determine an associated upper limit to the output power.

Using Eq. (1), the power lost in a cavity can be expressed as

$$P_n = \frac{Q_T}{Q_n} P_w, \quad (10)$$

where Q_T is the total ("loaded") Q , and Q_n is the Q due to ohmic losses in the cavity. P_w is the total power produced in the cavity. Q_T is given by

$$Q_T = (Q_n^{-1} + Q_0^{-1})^{-1}$$

where Q_0 is produced by the useful power coupled out of the cavity. For small losses, $Q_T \approx Q_0$. Q_n for TE_{on1} modes is given by⁽¹⁰⁾

$$Q_n = \frac{2\pi f \mu a}{2R} \left(\frac{\alpha_{1n}^2 L^2 + \pi^2 a^2}{\alpha_{1n}^2 L^2 + \frac{2\pi^2 a^3}{L}} \right). \quad (11)$$

R is the surface resistivity. Equation (11) is easily rearranged to

$$Q_n = \frac{2\pi f \mu a}{2R} \left(\frac{\alpha_{1n}^2 + \pi^2 a^2 2/L^2}{\alpha_{1n}^2 + \frac{2\pi^2 a^3}{L^3}} \right). \quad (12)$$

For gyrotron cavities $\alpha_{1n}^2 \gg \pi^2 a^2/L^2$. Then

$$Q_n = \frac{2\pi f \mu a}{2R}. \quad (13)$$

Inserting values for $\mu = \mu_0 = 4\pi \cdot 10^{-7} H/m$ and the surface resistance of copper, we find

$$Q_n = 15.2 f^{1/2} a \quad (\text{MKS units}) \quad (14)$$

As before, we can express the wall radius a in terms of λ and the zero of the Bessel function J_1 . Then

$$Q_n \approx 15.2 \left(\frac{L}{\lambda} \right)^{1/2} \frac{\lambda \alpha_{1n}}{2\pi}$$

or

$$Q_n \approx 4.19 \cdot 10^4 \lambda^{1/2} \alpha_{1n}. \quad (15)$$

Using as before, the lower limit of $Q_0 = 2Q_D$ we find

$$\frac{P_\Omega}{P_w} \approx \frac{Q_0}{Q_\Omega} = \frac{6.0 \cdot 10^{-4}}{\alpha_{1n}} \frac{L^2}{\lambda^{5/2}}$$

or

$$\frac{P_\Omega}{P_w} \approx \frac{3.46 \cdot 10^{-8}}{\alpha_{1n}} f^{1/2} \frac{L^2}{\lambda^2}. \quad (16)$$

If the assumption that $Q_0 \ll Q_\Omega$ is not valid, the expression of interest is

$$\frac{P_\Omega}{P_w} = \frac{Q_\Omega}{Q_T} = \left(1 + \frac{Q_\Omega}{Q_0}\right)^{-1}. \quad (17)$$

The values of P_Ω/P_w from Eq. (16) as a function of L/λ for several modes at $f = 100$ GHz are given in Fig. 4.

For cavity wall heating, the average power loss per unit area is of interest. This is given by

$$\frac{P_\Omega}{A} \approx \frac{P_w}{2\pi aL} \cdot \frac{3.46 \cdot 10^{-8}}{\alpha_{1n}} f^{1/2} \frac{L^2}{\lambda^2} \left(1 + \frac{Q_0}{Q_\Omega}\right)^{-1}. \quad (18)$$

The cavity surface area, A , can be given by $2\pi aL$ since, for TE_{on1} modes near cutoff, the losses are primarily in the side walls of the cavity.

Equation (18) reduces, with the assumption that $Q_0 \ll Q_\Omega$, to

$$\frac{P_\Omega}{A} = \frac{3.84 \cdot 10^{-25}}{\alpha_{1n}^2} f^{5/2} \frac{L}{\lambda} P_w \quad (19)$$

or

$$\frac{P_\Omega}{A} = 4.18 \cdot 10^{-13} f^{5/2} \frac{J_2^2(\alpha_{1n})}{J_1^2\left(\alpha_{1n} \frac{b}{a}\right)} \mathcal{G}_b^2 \quad (20)$$

Using Eq. (19), plots of the average wall heating per unit area versus L/λ for various TE_{on1} modes at $f = 100$ GHz have been produced, and are shown in Figs. 5a, b, c and d. The power densities given here will be clearly scaled by the same factors for beam location as for the total cavity power.

LOWER LIMITS ON THE OUTPUT POWER

The lower limit on the power of a gyromonotron (assuming, again, that we operate at optimum efficiency for a given length) is determined by the tolerable wall losses.

Using Eq. (1), we can write

$$P_0 = \frac{\epsilon_0 c^3}{4Q_0} \frac{L}{\lambda} \alpha_{1n}^2 \frac{J_2^2(\alpha_{1n})}{J_1^2\left[\alpha_{1n} \frac{b}{a}\right]} g_b^2 \quad (21)$$

The upper bound for Q_0 , the output Q , is determined by the severity of the wall losses that can be tolerated. For, as above,

$$\frac{P_\Omega}{P_w} = \frac{Q_T}{Q_\Omega} = \frac{Q_0}{Q_0 + Q_\Omega}$$

or

$$Q_0 = \frac{P_\Omega}{P_w} \left(1 - \frac{P_\Omega}{P_w}\right)^{-1} Q_\Omega \quad (22)$$

Let

$$B \equiv \frac{P_\Omega}{P_c} \left(1 - \frac{P_\Omega}{P_w}\right)^{-1}$$

Then

$$P_0 = \frac{\epsilon_0 c^3}{4BQ_\Omega} \frac{L}{\lambda} \alpha_{1n}^2 \frac{J_2^2(\alpha_{1n})}{J_1^2\left[\alpha_{1n} \frac{b}{a}\right]} g_b^2. \quad (23)$$

Inserting Q_Ω from equation (14), we find

$$(P_0)_{\min} = \frac{8.28 \cdot 10^4}{B} f^{1/2} \alpha_{1n} \frac{J_2^2(\alpha_{1n})}{J_1^2(\alpha_{1n} \frac{b}{a})} \frac{L}{\lambda} g_b^2 \quad (24)$$

We note that $(P_0)_{\min}$ is essentially independent of the mode (for a given beam placement) since $\alpha_{1n} J_2^2(\alpha_{1n})$ is approximately constant. The largest difference occurs between the TE₀₁ and TE₀₂ modes (approximately 4%). The power for the TE₀₃ and higher modes can be approximated by the TE₀₂ results.

$B \cdot P_0$, for a frequency of 100 GHz, as a function of L/λ , is plotted in Fig. 6a and b.

COMPARISON TO EXPERIMENT

Experimental data reported elsewhere^(12,13) can be used to check the validity of the calculations for the maximum power for the TE₀₁₁ mode. This data is plotted in Fig. 7. The actual powers

observed in the experiments have been multiplied by the measured Q_L divided by $2Q_D$ since the cavities used in the experiments had values for Q_L not necessarily equal to $2Q_D$. No magnetic tapering was used in obtaining these points. (Interpretation of the data with tapering is somewhat complicated by details of the experiment, and is given in Reference 11.) Within experimental error, the agreement of experiment and theory for the data given in Fig. 8 appears quite good.

COMMENTS

All of the power limits have been derived for operation where, for a given length, the efficiency is optimized. The fall-off of efficiency with increasing RF electric field amplitude is fairly gradual, and some increase in power can be obtained by "overdriving" a cavity. An example of efficiency versus beam power is given in Fig. 8.

A much more substantial increase in power may be obtained by overdriving the cavity so that the beam electrons go through a complete trapping cycle⁽¹¹⁾, so that they, on the average, lose, then gain, then again lose energy to the wave.⁽¹²⁾ Initial theoretical investigations indicate that a factor of 10 increase in the power may be possible with this method. This would allow the use of a long cavity ($L/\lambda \approx 8$) where relatively modest magnetic field gradients are required, to produce the same power (at equivalent efficiencies) as a shorter cavity, which would require possibly unrealizable gradients. This possibility will be the subject of future studies.

CONCLUSIONS

We have presented scaling factors useful in the design of gyromonotrons. In particular, we have given an electric field magnitude, normalized to the frequency, which can be used to determine the output power for any TE_{on1} mode. This field should be applicable to coaxial, as well as to the open cylindrical geometry.

For the open cylindrical cavities, it is clear that there are definite bounds on gyromonotron output powers. For very high frequencies, these bounds may become severe. For example, at 100 GHz, it is

READ, CHU, AND KIM

impossible to find an operating power for an optimum length cavity ($\frac{L}{\lambda} = 8$) using the TE_{011} mode, and losing less than 20% of the power to ohmic losses.

For CW operation ohmic losses will limit the maximum power. It is clear from Figs. 3 and 5 that powers over 1 MW will cause power dissipation above 1 kW/cm² even when using a relatively high order mode of TE_{051} . This limit is valid even when using the beam position enhancement factors, and therefore will serve as an ultimate upper bound. We note that these limits are optimistic, since it is in practice difficult to realize the calculated ohmic Q . A more practical limit on the output powers may be obtained by doubling the ohmic losses given in Figs. 4 and 5. Some advantage may be obtained by reducing the ohmic losses to cooling the cavity to liquid nitrogen (or lower) temperatures, but it seems unrealistic to expect operation of a single gyromonotron using an open cylindrical cavity at above a few MW.

ACKNOWLEDGMENTS

The authors would like to thank Dr. B. Arfin and Dr. V. L. Granatstein for their useful comments.

This work was supported by the Department of Energy, Contract #DE-AC01-79ET52053.

References

1. V.V. Alikoaev *et al.* *Fiz Plasmy* **2**, 390 (1976) *Soviet Journal of Plasma Physics* **2**, 212 (1976).
2. R.M. Gilgenbach *et al.* *Phys. Rev. Letters* **44**, p. 647 (1980).
3. E. Ott, B. Hui, and K.R. Chu, *Phys. Fluids* (to be published).
4. R.J. Temkin, K.E. Kreischer, V. Schultz, and D.R. Cohn, *MIT Plasma Fusion Center Rpt. PFC/RR-79-20* (1979).
5. At present the highest power CW source is the 28 GHz, 212 kW Varian Associates gyromonotron.

NRL MEMORANDUM REPORT 4349

6. K.R. Chu, M.E. Read, and A.K. Ganguly, IEEE Trans. MTT (in press, April, 1980).
7. V.L. Bratman, M.A. Moiseev, M.I. Petelin and R.E. Erm, Radiophysics and Quantum Electronics, 16 (1973).
8. S.N. Vlasov, L.I. Zagryadskaya, and M.I. Petelin, Radiophysics and Quantum Electronics, 16, 11.
9. M. Abramowitz and I. Stegun, "Handbook of Mathematical Functions," Dover Publications, New York, pp. 390-396 (1965).
10. S.A. Schelkenoff, "Electromagnetic Waves," D. Van Nostrand Co., Inc., Princeton, N.J. (1943).
11. P. Sprangle and A.T. Drobot, IEEE Trans. on Microwave Theory and Techniques, MTT-25, 1977.
12. M.E. Read, K.R. Chu, and A.J. Dudas, to be published.
13. M.E. Read, R.M. Gilgenbach, A.J. Dudas, R. Lucey, K.R. Chu, and V.L. Granatstein, Proceedings of the IEEE 4th International Conference on Infrared and Millimeter Waves and their Applications, Miami, Fl. Dec. 1979.

**Table 1. Power Enhancement Factors For Beam Placements
On Higher Order Peaks of the Electric Field**

Peak #	Enhancement*
1	1
2	2.83
3	4.54
4	6.24
5	7.91

*Equal to $\frac{J_1^2(\beta_1)}{J_1^2(\beta_p)} \cdot J_1^2(\beta_1)$ is the value of J_1^2 at its first peak and $J_1^2(\beta_p)$ is the value of J_1^2 for the p^{th} maximum. Values of J_1 from reference (9).

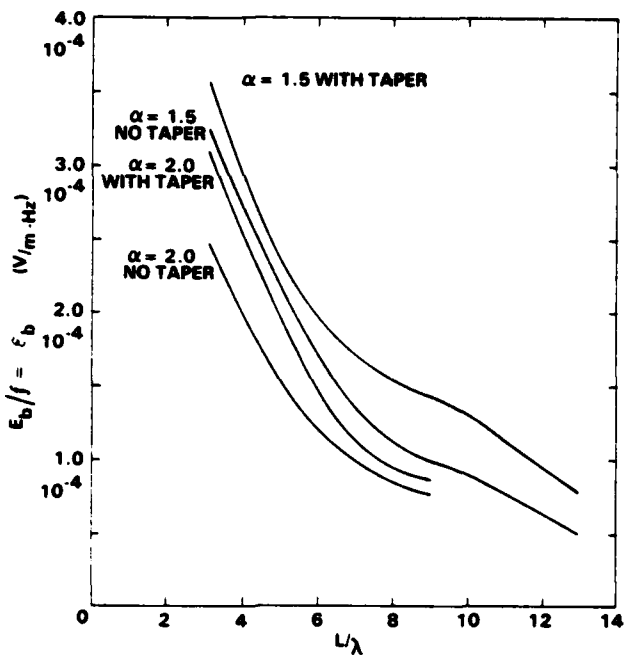


Fig. 1 — Optimum electric field at the beam location (normalized to the frequency) for optimum efficiency as a function of normalized cavity length. Curves are given for two values of α with and without optimal values of magnetic tapering.

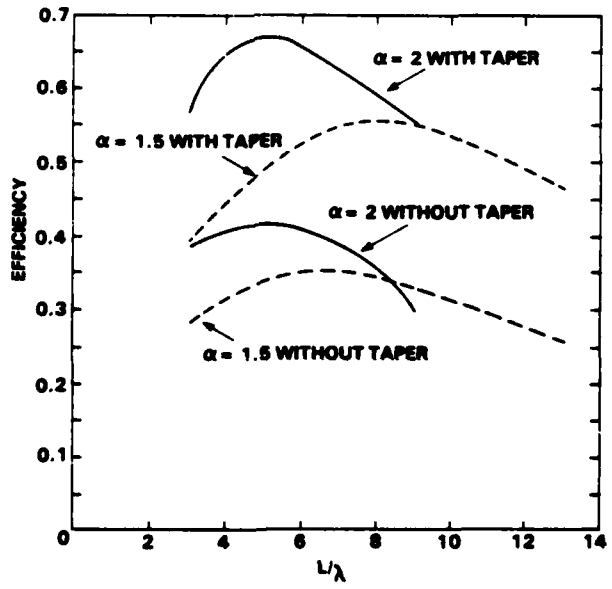


Fig. 2 — Efficiency versus normalized cavity length, for the conditions of Fig. 1

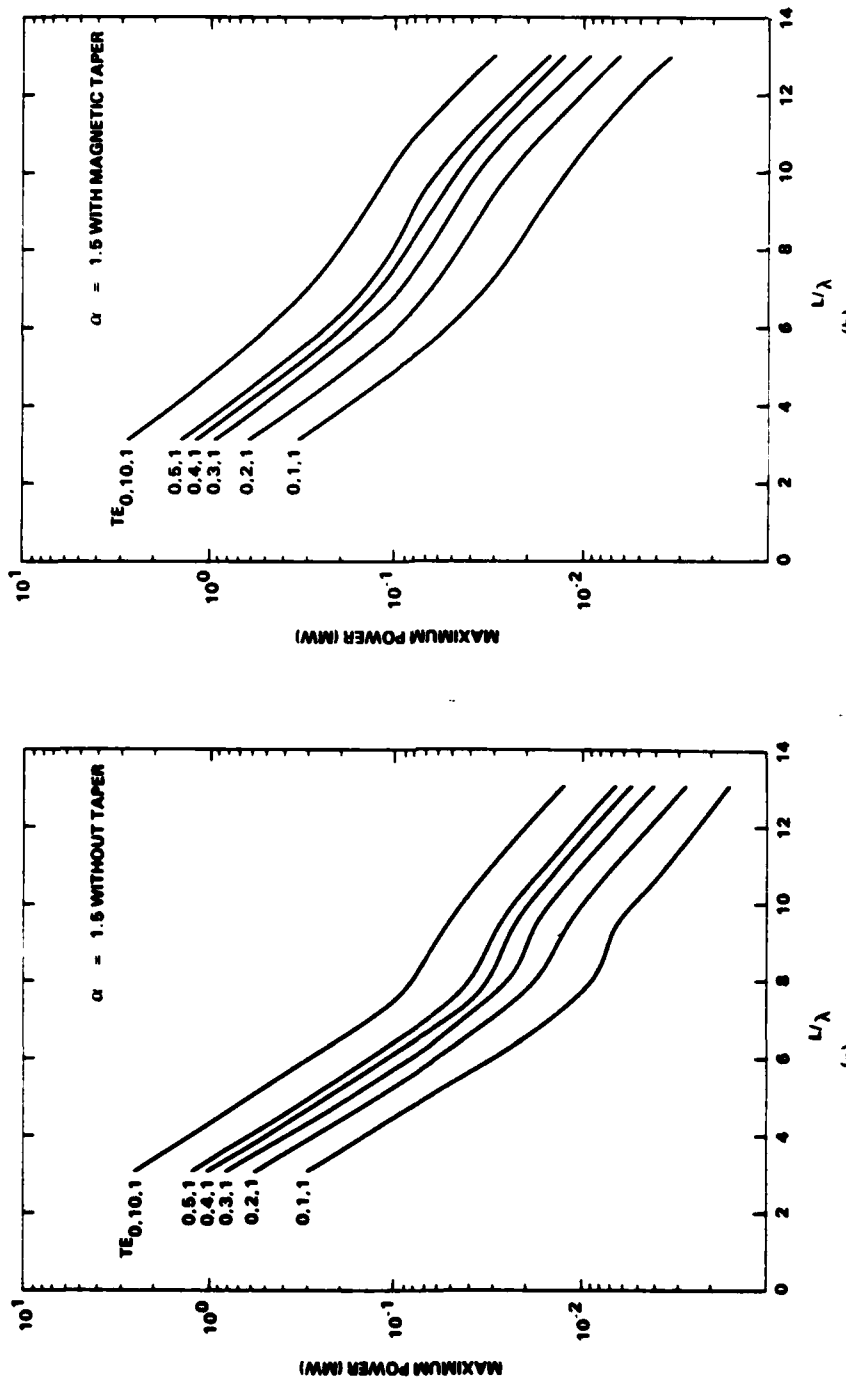


Fig. 3 — Maximum output power for $Q = 2Q_D$ versus normalized cavity length (a) $\alpha = 1.5$, with magnetic taper, (b) $\alpha = 1.5$ without magnetic taper, (c) $\alpha = 2.0$ without magnetic taper, and (d) $\alpha = 2.0$ with magnetic taper

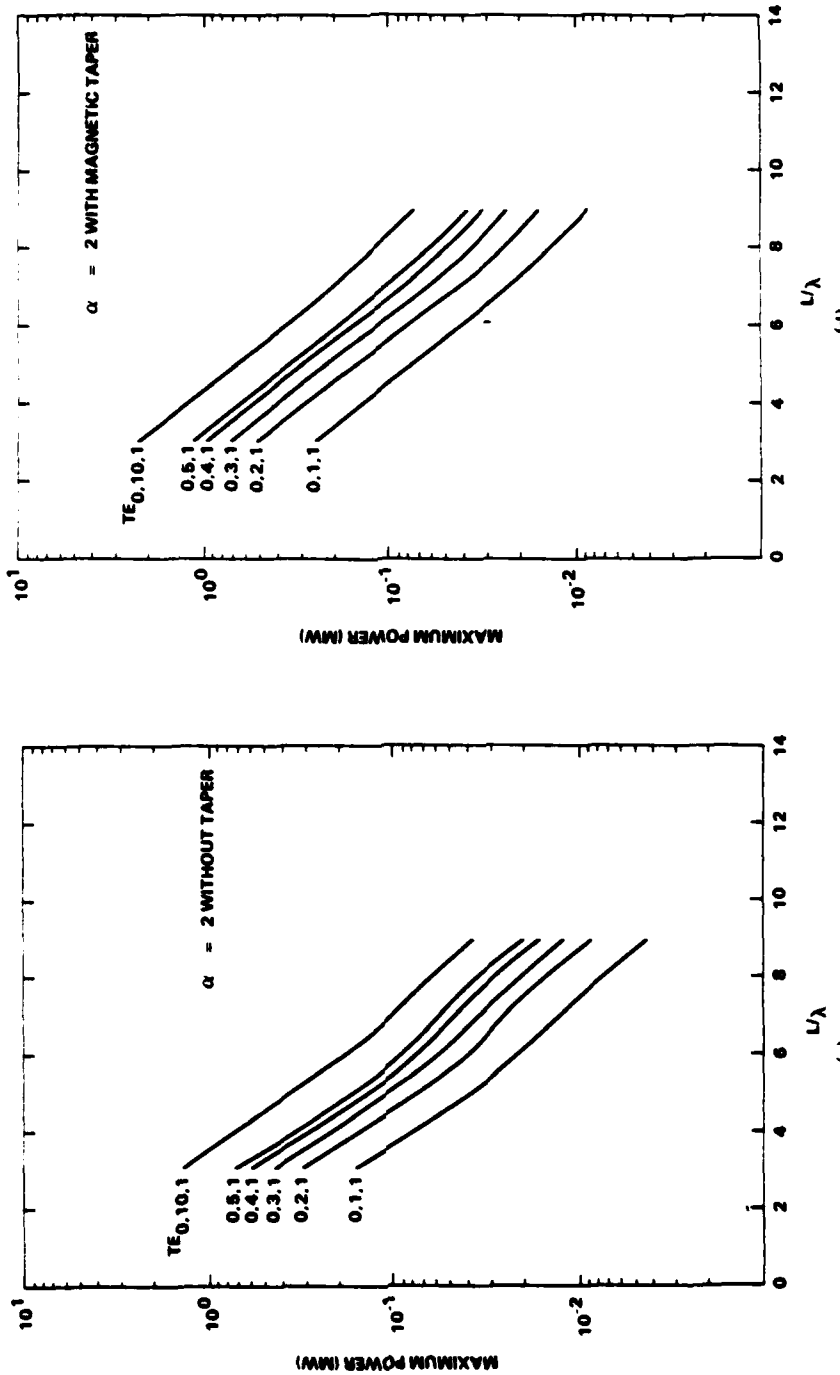


Fig. 3 (Continued) — Maximum output power for $Q = 2Q_b$ versus normalized cavity length (a) $\alpha = 1.5$, without magnetic taper, (b) $\alpha = 1.5$ with magnetic taper, (c) $\alpha = 2.0$ without magnetic taper, and (d) $\alpha = 2.0$ with magnetic taper.

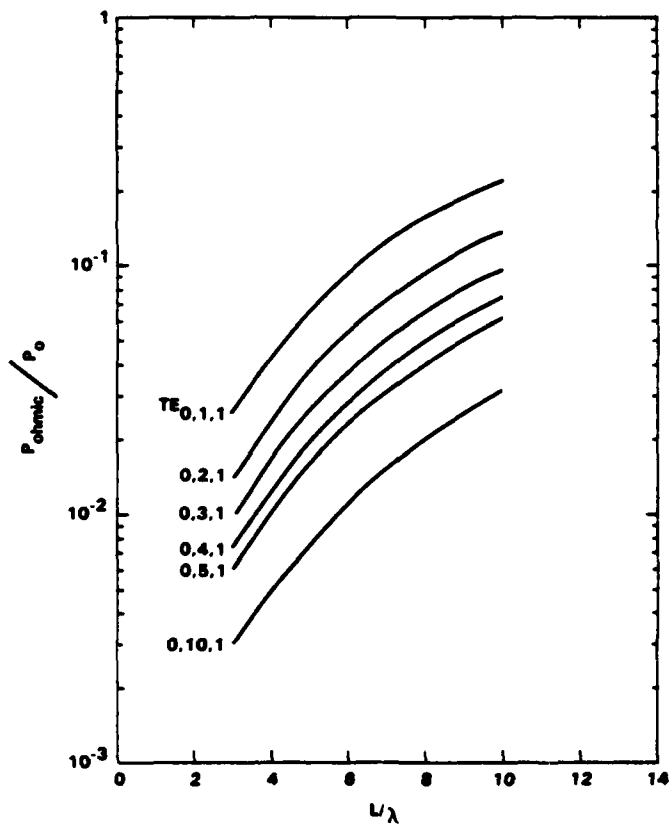


Fig. 4 — Ratio of ohmic losses to total cavity power as a function of normalized cavity length for a frequency of 100 GHz

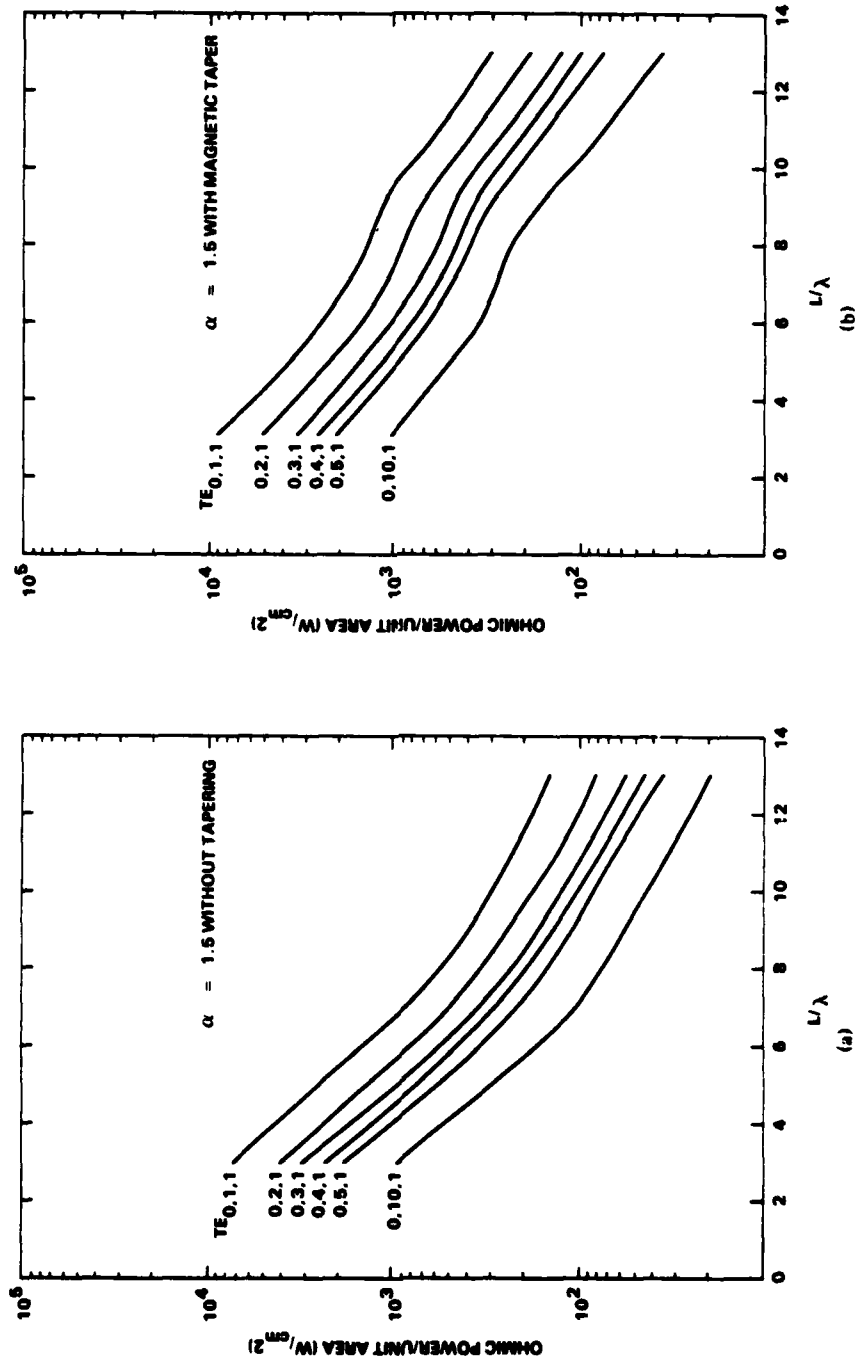


Fig. 5 — Ohmic power dissipation, per unit area, as a function of normalized cavity length. (a) $\alpha = 1.5$, without magnetic taper.
 (b) $\alpha = 1.5$ with magnetic taper. (c) $\alpha = 2.0$ without magnetic taper, and (d) $\alpha = 2.0$ with magnetic taper

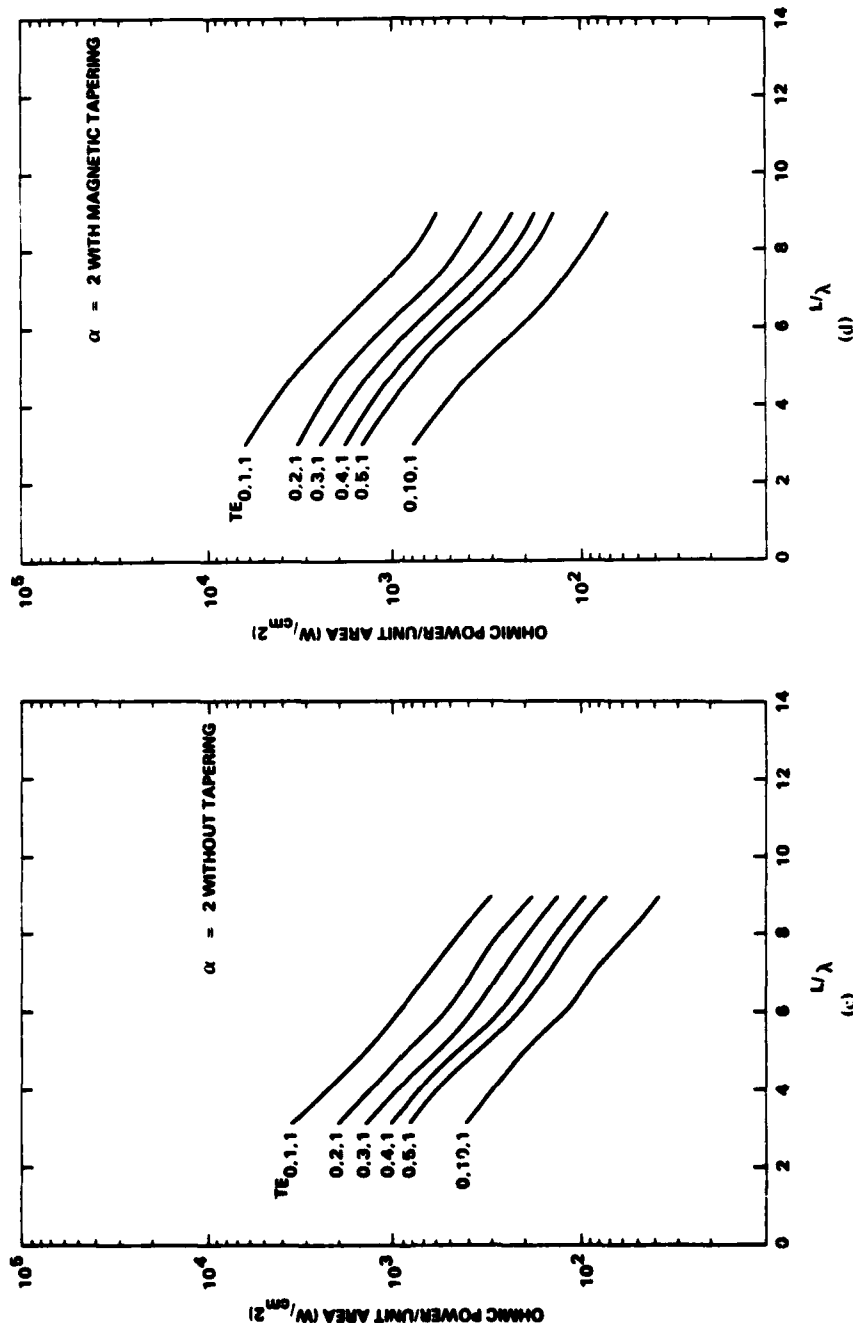


Fig. 5 (Continued) — (Ohmic power dissipation, per unit area, as a function of normalized cavity length. (a) $\alpha = 1.5$, without magnetic taper, (b) $\alpha = 1.5$ with magnetic taper, (c) $\alpha \approx 2.0$ without magnetic taper, and (d) $\alpha = 2.0$ with magnetic taper

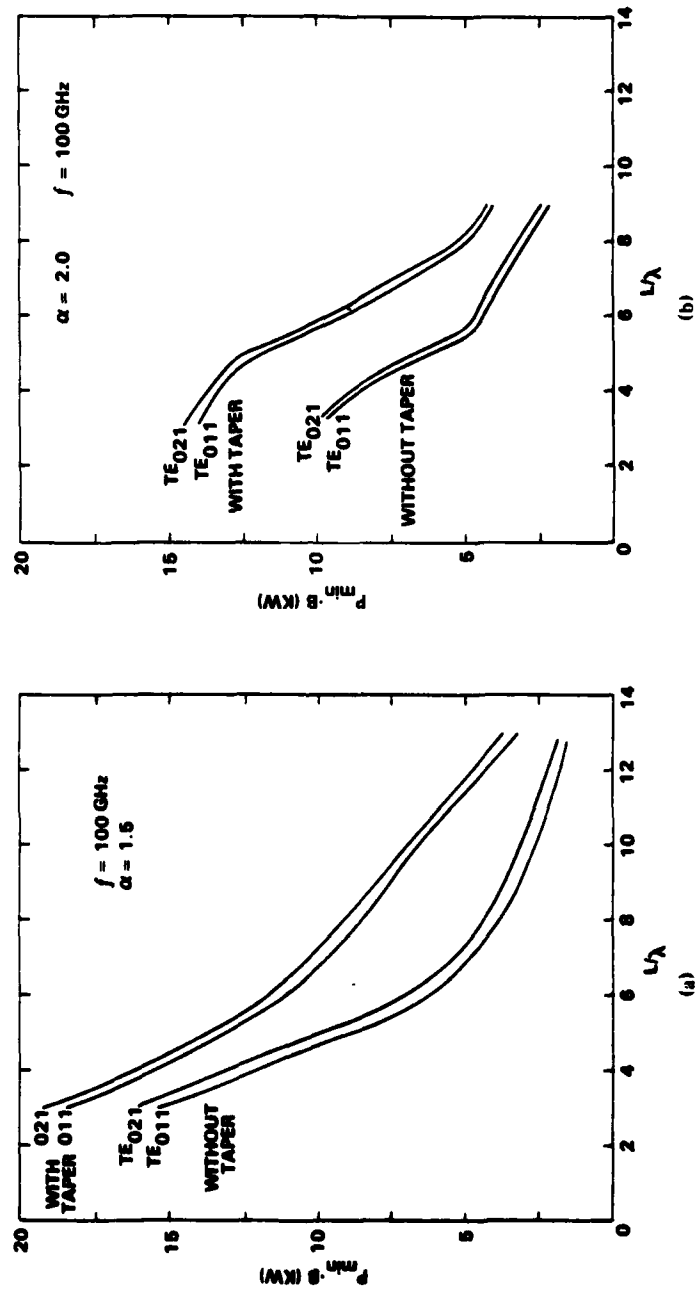


Fig. 6 — Normalized minimum output power as a function of the normalized cavity length,
for a frequency of 100 GHz (a) $\alpha = 1.5$; (b) $\alpha = 2.0$

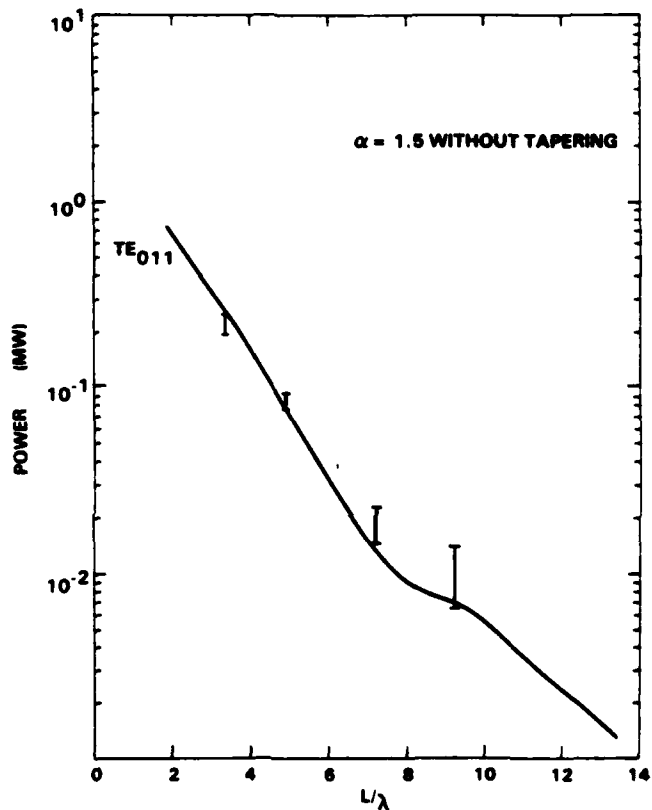


Fig. 7 — Output power versus cavity length for the TE_{011} mode. Experimental points and the theoretical curve from Figure 3a are given. The actual experimentally observed powers have been multiplied by $Q_{\text{observed}}/2Q_D$ for comparison with theory. No magnetic taper was used in the experiments.

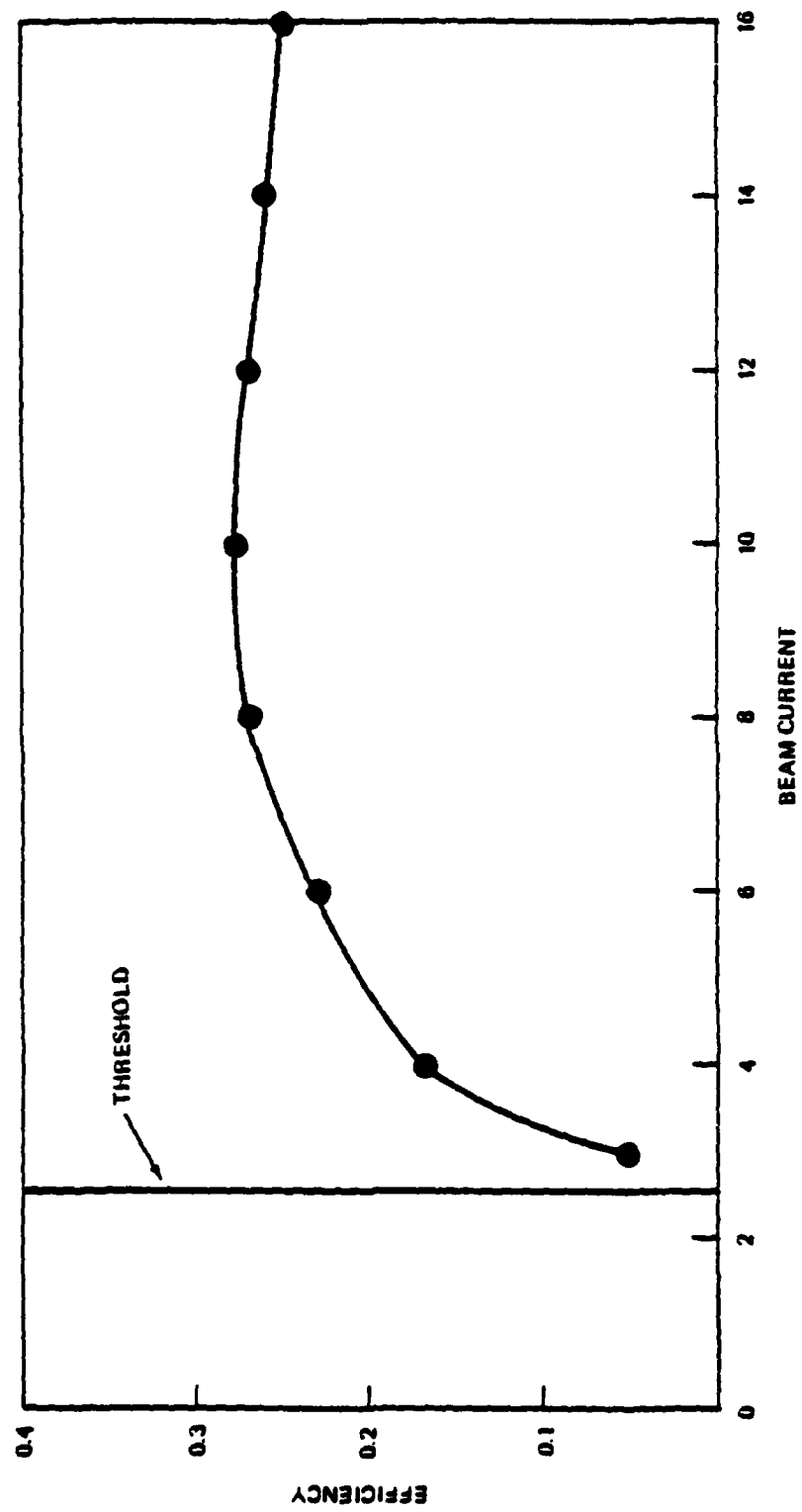


Fig. 8 - A "typical" efficiency versus beam current plot ($V = 70$ kV, $Q = 400$, $L/\lambda = 3.3$, mode = TE_{01}).

GYROTRON & ECH DISTRIBUTION LIST

No. of Copies

(25) Naval Research Laboratory
(26) Attn: Name/Code
4555 Overlook Avenue, S.W.
Washington, D.C. 20375

Addressee

Code: 4700 - Dr. T. Coffey
4740 - Dr. V.L. Granatstein
4740 - Dr. R.K. Parker
4740 - Dr. K.R. Chu
4740 - Dr. M.E. Read
4740 - Dr. C.W. Roberson
4740 - Dr. S. Gold
4790 - Dr. P.A. Sprangle
4790 - Dr. B. Hui
4790 - Dr. W.M. Manheimer
6850 - Dr. L.R. Whicker
6853 - Dr. A. Ganguly
6805 - Dr. S.Y. Ahn
6805 - N.R. Vanderplaats
6875 - Dr. R. Wagner

On-Site Contractors:

Code: 4740 - Dr. J.M. Baird (B-K Dynamics)
4740 - Dr. L. Barnett (B-K Dynamics)
4740 - Dr. D. Dialetis (SAI)
4740 - A.J. Dudas (JAYCOR)
4740 - Dr. R.M. Gilgenbach (JAYCOR)
4740 - Dr. K.J. Kim (JAYCOR)
4740 - Dr. Y.Y. Lau (SAI)
4740 - Dr. J.S. Silverstein (HDL)
4790 - Dr. A.J. Drobot SAI
4790 - Dr. C.M. Hui (JAYCOR)
4790 - Dr. J. Vomvoridis (JAYCOR)
5704S - Dr. S. Smith (LOCUS, Inc.)

(3) Secretary
Department of Energy
Attn:
Washington, D.C. 20545

Dr. P. Stone (G-234)
Dr. M. Murphy (G-234)
Dr. J. Willis (G-234)

(1) Air Force Avionics Laboratory
Attn: W. Friz
Wright/Patterson AFB, Ohio 45433

(1) Bell Laboratories
Attn: Dr. W.M. Walsh, Jr.
600 Mountain Avenue
Murray Hill, New Jersey 07971

PRECEDING PAGE BLANK-NOT

<u>No. of Copies</u>	<u>Addressee</u>
(1) Columbia University Department of Electrical Engineering Attn: Dr. S.P. Schlesinger New York, New York 10027	
(1) Dartmouth College Physics Department Attn: Dr. John Walsh Dartmouth, New Hampshire 03755	
(12) Defense Technical Information Center Cameron Station 5010 Duke Street Alexandria, Virginia 22314	
(1) Georgia Institute of Technology Engineering Experimental Station Attn: Dr. James J. Gallagher Atlanta, Georgia 30332	
(3) Hughes Aircraft Co. Attn: Electron Dynamics Division 3100 Lomita Boulevard Torrance, California 90509	Dr. J.J. Tancredi K. Arnold K. Amboss
(1) Los Alamos Scientific Laboratory Attn: Dr. Paul Tallerico P.O. Box 1663 Los Alamos, New Mexico 87545	
(1) Massachusetts Institute of Technology Research Laboratory of Electronics Attn: Dr. G. Bekefi Bldg. 36, Rm. 36-225 Cambridge, Massachusetts 02139	
(3) Massachusetts Institute of Technology Plasma Fusion Center Attn: 167 Albany St., N.W. 16-200 Cambridge, Massachusetts 02139	Dr. R. Davidson Dr. M. Porkolab Dr. R. Temkin
(1) Northrop Corporation Defense System Department Electronics Division Attn: G. Doehler 175 W. Oakton St. Des Plaines, Illinois 60018	
(2) Oak Ridge National Laboratories Attn: P.O. Box Y Oak Ridge, Tennessee 37830	Dr. A. England M. Loring

<u>No. of Copies</u>	<u>Addressee</u>
(1) Princeton University Plasma Physics Laboratory Attn: Dr. H. Hsuan Princeton, New Jersey 08540	
(2) Raytheon Company Microwave Power Tube Division Attn: Willow St. Waltham, Massachusetts 02154	R. Edwards R. Handy
(1) Science Applications, Inc. Attn: Dr. Alvin Trivelpiece 1200 Prospect St. La Jolla, California 92037	
(1) Stanford University SLAC Attn: Dr. Jean Lebacqz Stanford, California 94305	
(1) University of Arizona Optical Sciences Center Attn: Dr. W.E. Lamb Tucson, Arizona 85720	
(1) Varian Associates Bldg. 1 Attn: Dr. H. Jory 611 Hansen Way Palo Alto, California 94303	
(1) Yale University Mason Laboratory Attn: Dr. J.L. Hirshfield 400 Temple Street New Haven, Connecticut 06520	
(1) Kings College University of London Attn: Dr. P. Lindsay London, United Kingdom	
(1) Nagoya University Institute of Plasma Physics Attn: Dr. H. Ikegami Nagoya, Japan 464	
(1) National Taiwan University Department of Physics Attn: Dr. Yuin-Chi Hsu Taipei, Taiwan, China	

<u>No. of Copies</u>	<u>Addressee</u>
(1)	TFR Group DPH - PFC Attn: Dr. A. Cavallo 92260 Fontenay-aux Roses France
(1)	Thompson C.S.F./DET/TDH Attn: Dr. G. Mourier 2 Rue Latecoere 78140 Velizy Villa conblay France
(1)	UKAEA Culham Laboratory Attn: Dr. A.C. Riviere Abingdon Oxfordshire United Kingdom

DATE
FILMED
- 8